

New mechanism for spin effects in large-angle N - N elastic scattering

C. Bourrely and J. Soffer

Centre de Physique Théorique, Centre National de la Recherche Scientifique, Luminy Case 907, 13288 Marseille Cedex 9, France

(Received 17 September 1986)

In the framework of a simple physical approach we show that the amplitudes generated by hard scattering can interfere with the diffractive amplitudes giving a new mechanism which describes both the elastic p - p differential cross section and the analyzing power at large angles and high energy. In view of future experiments we present the model predictions for different two-spin parameters in p - p and p - n elastic scattering. If one tries to apply the same mechanism by using perturbative QCD it fails and one can speculate about the presence of higher-twist-effect contributions which remain to be evaluated.

I. INTRODUCTION

Over the last 15 years or so the role of spin effects in hadron physics was considered as having a rather minor interest for a comprehensive understanding of hadron structure. This prejudice was supported by the difficulty involved in the theoretical developments and also by the fact that most of the experimental results for exclusive processes were obtained at an energy of a few GeV and small-angle scattering. Nevertheless the accumulation of data during this period shows many large unexpected spin effects^{1,2} which are not completely understood. This energy and momentum-transfer region refers to the so-called "soft" physics domain which is described by phenomenological models,³ but probably not in the framework of perturbative QCD (PQCD), considered to be the standard theory for strong-interactions dynamics. In order to test PQCD and our knowledge of color-quark dynamics at very short distances one needs experimental data at large momentum transfer and high energy. After the Zero Gradient Synchrotron at Argonne was shut down, a program for accelerating polarized protons up to 26 GeV/ c was undertaken at the Brookhaven Alternating Gradient Synchrotron and as a result of a considerable successful work, it is now ready to discover new spin effects. Meanwhile the analyzing power A for p - p elastic scattering was measured at 28 GeV/ c with a polarized target⁴ for a p_T ² up to 6.5 GeV², and a rapid increase of A close to 24% has been observed at the largest p_T , an effect which was not anticipated. This is shown in Fig. 1, where the observables A and A_{NN} , the transverse spin-spin correlation parameter, are plotted versus p_{lab} at fixed c.m. angle ($\theta \approx 50^\circ$). It also shows a recent result obtained from the BNL polarized beam at 18.5 GeV/ c (Ref. 5). The appearance of a new regime in p - p collisions for $P_{lab} > 20$ GeV/ c is clearly seen for A , and in the case of A_{NN} a new measurement at 28 GeV/ c is led for.

These results suggest that spin effects in exclusive p - p scattering at high energy and large angles are important, so we have to find a mechanism which can generate such a large value of A and also to show its relation to the basic quark asymmetries in different models. In the next

section we discuss such a possible mechanism in the context of a simple physical quark model and the predictions for different spin correlation parameters are presented. A similar analysis is made for the case of PQCD and related models in Sec. III, and we give our concluding remarks in Sec. IV.

II. AN INTERFERENCE MECHANISM BETWEEN DIFFRACTIVE AND HARD SCATTERING

p - p and \bar{p} - p elastic scattering at small angles are well described by a model based on a new impact picture for

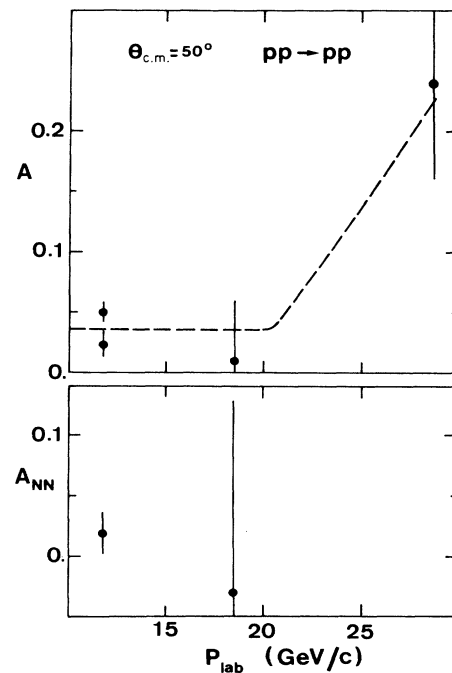


FIG. 1. p - p polarization parameters A and A_{NN} vs p_{lab} for fixed c.m. angle $\theta \approx 50^\circ$ (data from Refs. 4–6). The dashed line is hand-drawn to guide the eye.

low and high energy⁷ which gives a satisfactory phenomenological analysis of the unpolarized cross sections from CERN PS up to SPS collider energy⁸ and also for the analyzing power A at high energies.⁹ The scattering amplitudes generated by this model provide an accurate representation of the soft-scattering process at small angles, and in particular it allows a good description of the differential cross section at the PS energy for a momentum transfer up to 4 GeV^2 as shown in Fig. 2. Beyond this value the diffractive contribution drops more rapidly than the experimental data, giving a clear indication that a hard-scattering effect becomes dominant at large angles and should be included to complete the physical picture.

Large-angle two-body hadron scattering has been analyzed in terms of various hard-scattering models either based on PQCD or in the framework of quark geometrodynamics (QGD) and its more refined version anisotropic chromodynamics.¹⁰ For all these approaches the helicity amplitudes are essentially real, so by taking only the hard-scattering contribution at large angles the analyzing power A will be zero due to the absence of a phase difference [see Eq. (4) below]. However, the diffractive nonflip amplitude which is mainly imaginary and only dominant at small angles can be sizable enough at large angles to allow a maximum interference effect with the real hard spin-flip amplitude producing a nonzero analyzing power. This is precisely the mechanism we will advocate in the following¹¹ and we will propose further tests for it.

The QGD-ACD approach¹⁰ provides a theoretical framework to compute the basic quark-quark scattering amplitudes, the quark wave function of the low-lying hadron spectrum and the large-angle hadron-hadron scattering amplitudes.¹²⁻¹⁴ The model, which has quark confinement explicitly built in, is based on the following phenomenological hypothesis: hadrons are made out of a small number of quarks which form the primitive states and are confined in simple space-time domains whose dimensions increase linearly with the mass of the hadronic states. Furthermore the number of quarks involved in an hadronic process obeys a perturbative structure and the

hadrons produced in the final states result from the decay of a perturbative evolution of the above primitive states.

The two-body large-angle hadron-hadron amplitudes are obtained by folding the hadron vertex functions with the elementary quark-quark and quark-diquark scattering amplitudes.¹³ The vertex functions are constructed under the assumption that during the scattering process the initial and final baryons have in common two spectators quarks which conserve spin, momentum, and the internal degrees of freedom. At the level of the basic quark-quark scattering amplitudes it is assumed that the short-distance force (which is color neutral) is generated by the exchange of several infinite towers of mesons, which are not only transverse vector states (analogous to gluons in PQCD), but also pseudoscalar and longitudinal vector states. As a consequence, the spin structure of the quark-quark amplitudes is not as restrictive as that of PQCD which conserves helicity.

The QGD-ACD helicity amplitudes for nucleon-nucleon scattering in the isospin $I=1$ and 0 states are given in Table I, they differ slightly from those in Ref. 13 because we have not made the approximation of large-angle and high-energy limit. In particular the energy dependence of the quark-quark scattering amplitude, e.g., $G(t,u)$ which was approximated by $\ln(s/m_0^2)/(-u)^{3/2}$ must be instead,

$$\ln(1-2t/m_0^2)/(-u+1/R_T^2)^{3/2},$$

where R_T is the fixed transverse "size" of the meson states and it is reasonable¹⁰ to choose $R_T^2=4 \text{ GeV}^{-2}$. m_0 is a typical hadronic mass and we will take $m_0^2=2 \text{ GeV}^2$. The energy dependence of the vertex functions was selected to recover the large- t behavior of the proton form factor that we approximated before by $1/t^2$. It should now be replaced by $1/(t-\mu^2)^2$ with $\mu^2=0.71 \text{ GeV}^2$. All these natural changes allow a reliable determination of the hard-scattering amplitudes away from 90° . For the p - p and n - p elastic scattering we have the following combination of isospin states:

$$\langle pp | \Phi_i | pp \rangle = \Phi_i^I = 1, \quad (1)$$

$$\langle pn | \Phi_i | pn \rangle = \frac{1}{2}(\Phi_i^I = 1 + \Phi_i^I = 0). \quad (2)$$

In terms of the helicity amplitudes we express the differential cross section and the spin asymmetries as³

$$\sigma_0 = s^2 d\sigma/dt \\ = \frac{1}{2} (|\Phi_1|^2 + |\Phi_2|^2 + |\Phi_3|^2 + |\Phi_4|^2 + 4|\Phi_5|^2), \quad (3)$$

$$A = \text{Im}[(\Phi_1 + \Phi_2 + \Phi_3 - \Phi_4)\Phi_5^*]/\sigma_0, \quad (4)$$

$$A_{NN} = \text{Re}(\Phi_1\Phi_2^* - \Phi_3\Phi_4^* + 2|\Phi_5|^2)/\sigma_0, \quad (5)$$

$$D_{NN} = \text{Re}(\Phi_1\Phi_3^* - \Phi_2\Phi_4^* + 2|\Phi_5|^2)/\sigma_0, \quad (6)$$

$$K_{NN} = \text{Re}(\Phi_3\Phi_2^* - \Phi_1\Phi_4^* + 2|\Phi_5|^2)/\sigma_0, \quad (7)$$

$$A_{LL} = -(|\Phi_1|^2 + |\Phi_2|^2 - |\Phi_3|^2 - |\Phi_4|^2)/\sigma_0, \quad (8)$$

$$A_{SS} = \text{Re}(\Phi_1\Phi_2^* + \Phi_3\Phi_4^*)/\sigma_0. \quad (9)$$

Taking the high-energy limit we obtain for the differential cross section the asymptotic expression

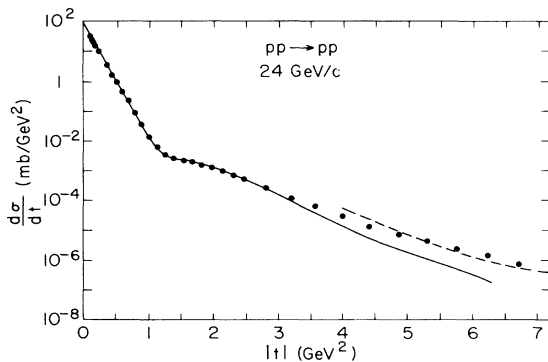


FIG. 2. p - p differential cross section for $p_{\text{lab}}=24 \text{ GeV}/c$. Solid curve, the diffractive model; dashed curve, diffractive QGD-ACD model (data from Ref. 15).

TABLE I. The helicity amplitudes $\Phi_j^I(s, \theta)$ for nucleon-nucleon scattering for isospin $I=1$ and $I=0$.

$I=1$
$\Phi_{1,2}(s, \theta) = s^{-9/2} [l_i G_{1,2}(\theta, t_\theta, u_\theta) + l_u G_{1,2}(\pi - \theta, u_\theta, t_\theta)]$ $\Phi_{3,4}(s, \theta) = s^{-9/2} [l_i G_{3,4}(\theta, t_\theta, u_\theta) - l_u G_{4,3}(\pi - \theta, u_\theta, t_\theta)]$ $\Phi_5(s, \theta) = s^{-9/2} [l_i G_5(\theta, t_\theta, u_\theta) - l_u G_5(\pi - \theta, u_\theta, t_\theta)]$ $t_\theta = 1 - \cos\theta + 2\mu^2/s, \quad u_\theta = 1 + \cos\theta + 2/(sR_T^2)$ $l_i = \ln(1 - 2t/m_0^2), \quad l_u = \ln(1 - 2u/m_0^2)$ <p>for $i=1,3, \epsilon_1=+, \epsilon_3=-$,</p> $G_i(\Phi) = \frac{[1 + \cos^2(\theta/2)](31 + 14 \cos\theta) + \epsilon_i 17 \sin^2(\theta/2)}{u_\theta^{3/2} t_\theta^2} + 6 \frac{(2 + \cos\theta)^2 + \sin^2\theta \sin^2(\theta/2)}{t_\theta^{7/2}}$ <p>for $i=2,4, \epsilon_2=+, \epsilon_4=-$</p> $G_i(\theta) = \epsilon_i \left\{ \frac{[1 + \cos^2(\theta/2)](31 - 14 \cos\theta) - \epsilon_i 17 \sin^2(\theta/2)}{u_\theta^{3/2} t_\theta^2} + 6 \frac{\sin^2\theta + \sin^2(\theta/2)(2 - \cos\theta)^2}{t_\theta^{7/2}} \right\}$ $G_5(\theta) = \frac{14 \sin\theta [1 + \cos^2(\theta/2)]}{u_\theta^{3/2} t_\theta^{3/2}} + 6 \frac{\sin\theta [2 + \cos\theta + \sin^2(\theta/2)(2 - \cos\theta)]}{t_\theta^{7/2}}$
$I=0$
$\Phi_{1,2}(s, \theta) = s^{-9/2} [l_i G_{1,2}(\theta, t_\theta, u_\theta) - l_u G_{1,2}(\pi - \theta, u_\theta, t_\theta)]$ $\Phi_{3,4}(s, \theta) = s^{-9/2} [l_i G_{3,4}(\theta, t_\theta, u_\theta) + l_u G_{4,3}(\pi - \theta, u_\theta, t_\theta)]$ $\Phi_5(s, \theta) = s^{-9/2} [l_i G_5(\theta, t_\theta, u_\theta) + l_u G_5(\pi - \theta, u_\theta, t_\theta)]$ <p>for $i=1,3, \epsilon_1=+, \epsilon_3=-$,</p> $G_i(\theta) = 3 \frac{[1 + \cos^2(\theta/2)](-1 + 10 \cos\theta) - \epsilon_i 11 \sin^2(\theta/2)}{u_\theta^{3/2} t_\theta^2} + 6 \frac{(2 + \cos\theta)^2 + \sin^2\theta \sin^2(\theta/2)}{t_\theta^{7/2}}$ <p>for $i=2,4, \epsilon_2=-, \epsilon_4=+$</p> $G_i(\theta) = \epsilon_i \left\{ 3 \frac{[1 + \cos^2(\theta/2)](1 + 10 \cos\theta) + \epsilon_i 11 \sin^2(\theta/2)}{u_\theta^{3/2} t_\theta^2} + 6 \frac{\sin^2\theta + \sin^2(\theta/2)(2 - \cos\theta)^2}{t_\theta^{7/2}} \right\}$ $G_5(\theta) = 6 \sin\theta \left\{ \frac{[1 + \cos^2(\theta/2)](5 + \cos\theta)}{u_\theta^{3/2} t_\theta^2} + \frac{2 + \cos\theta + \sin^2(\theta/2)(2 - \cos\theta)}{t_\theta^{7/2}} \right\}$

$$d\sigma/dt \rightarrow (1/s^{11}) \ln^2(s/m_0^2) F_{NN'}(\theta). \quad (10)$$

In this limit we notice a factorization property, i.e., a high negative power of the c.m. energy corrected by logarithmic terms, multiplied by a function of the scattering angle $F_{NN'}(\theta)$. This last function is given within an overall normalization factor which is fixed by comparison with the experimental value of the cross section at $\theta_{c.m.} = 90^\circ$.

The cross section for p - p elastic scattering at $p_{\text{lab}} = 24$ GeV/ c is shown with experimental data¹⁵ up to the highest momentum transfer 6.72 GeV² in Fig. 2; by adding the contributions of diffractive and hard-scattering amplitudes one gets a good agreement with the data, while the diffractive contribution alone drops too rapidly at large angle. At this point we would like to stress that the first test for the validity of a model is to agree with the

spin-average cross section. This minimal requirement is often ignored in the literature by models which give nevertheless predictions for spin observables.

According to the mechanism described above the spin asymmetries result from an interference effect between the QGD-ACD amplitudes and the spin-nonflip diffractive amplitudes which are strongly out of phase. We have deliberately omitted the diffractive spin-flip amplitudes to show clearly that the large values of A result from a maximum interference effect.¹⁶ This choice implies that for low-angle scattering ($\theta_{c.m.} < 40^\circ$) all the predicted spin observables cannot be compared to experiment, but a simple way to remedy this situation would be to include a spin-dependent Regge background as in Ref. 7. The calculated analyzing power for p - p at 28 GeV/ c in Fig. 3 shows a rapid increase for $\theta_{c.m.}$ between 40° - 46° to a maximum of

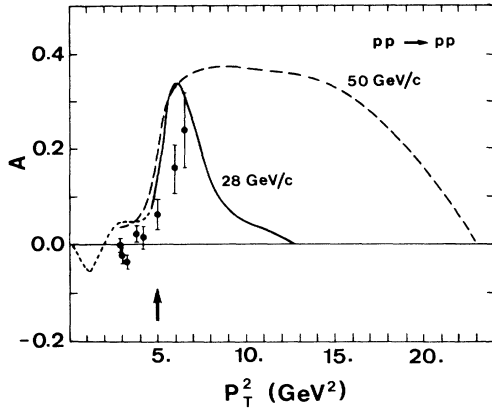


FIG. 3. Model predictions for p - p analyzing power at $p_{\text{lab}}=28$ and 50 GeV/c (data at 28 GeV/c from Ref. 4).

33%, which is to be compared with the average experimental value $(24 \pm 8)\%$ (Ref. 4). For $\theta_{\text{c.m.}} > 46^\circ$ A decreases sharply towards zero for $\theta_{\text{c.m.}} = 90^\circ$. The arrow indicates that below $p_T^2 = 5$ GeV², the broken line is not a reliable prediction at 28 GeV/c. At higher energy $p_{\text{lab}} = 50$ GeV/c, the predicted analyzing power has a large value over a broader p_T range and is certainly reliable down to $p_T^2 = 2$ GeV² or so, because as shown in Fig.

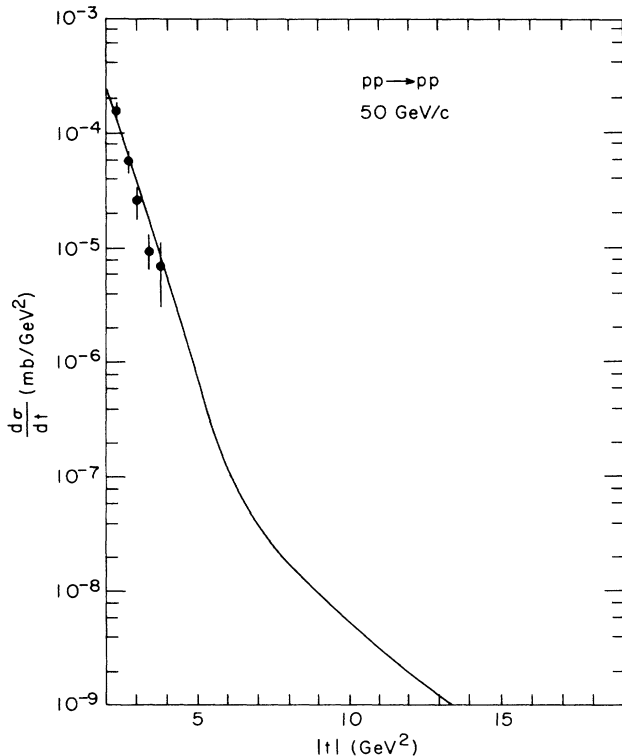


FIG. 4. p - p differential-cross-section data at large angles and 50 GeV/c from Ref. 17 compared to our model (diffractive + QGD-ACD).

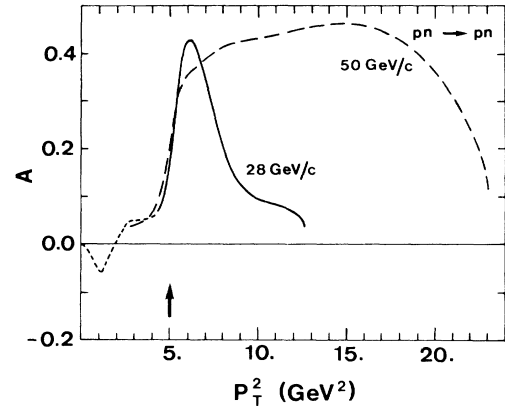


FIG. 5. Model predictions for p - n analyzing power at $p_{\text{lab}}=28$ and 50 GeV/c.

4 the cross section is well described down to smaller p_T^2 values.

For p - n elastic scattering the predicted A has a similar shape as for p - p , excepted that the maximum is now around 40% (Fig. 5). Note that the 6-GeV/c data shows a large *negative* A at large angles,¹⁸ so from our results we expect a rapid variation of A from negative to positive values in the energy range 6–28 GeV/c.

The A_{NN} asymmetry is shown in Figs. 6 and 7 for p - p and p - n elastic scattering at $p_{\text{lab}}=28$ and 50 GeV/c. They exhibit a continuous increase with the scattering angle and get close to 1 for $\theta_{\text{c.m.}} = 90^\circ$ at both energies. We notice that the experimental values of $A_{NN}(90^\circ)$ (Ref. 2) in the energy range 8–12 GeV/c are increasing up to 60%. We have also computed the K_{NN} asymmetry for p - p and p - n at $p_{\text{lab}}=28$ and 50 GeV/c (see Fig. 8). They have a behavior similar to A_{NN} . The D_{NN} asymmetry is almost constant at large angle and close to 1 at 90° , it nearly saturates the upper bound given by the inequalities:³

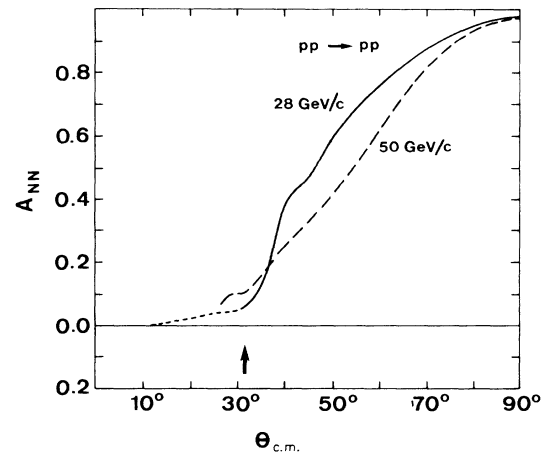


FIG. 6. Model predictions for A_{NN} vs $\theta_{\text{c.m.}}$ in p - p elastic scattering at $p_{\text{lab}}=28$ and 50 GeV/c.

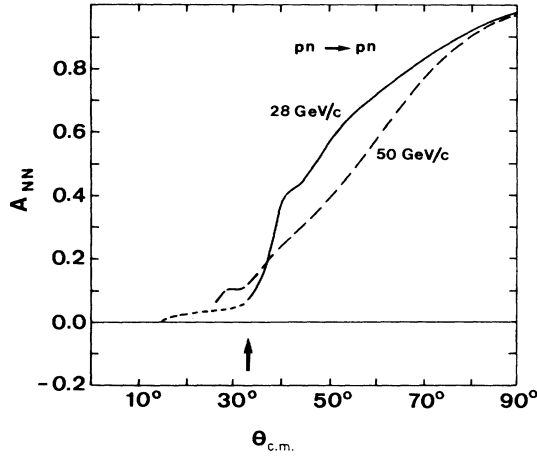


FIG. 7. Model predictions for A_{NN} vs $\theta_{c.m.}$ in p - n elastic scattering at $p_{lab}=28$ and 50 GeV/ c .

$$-\frac{1}{2}(1+A_{NN}) < D_{NN} < \frac{1}{2}(1+A_{NN}). \quad (11)$$

For large angles, A_{LL} is of the order of 2% while A_{SS} is around -4%, and the asymmetries satisfy at 90° the constraint³

$$1 - A_{NN} + A_{SS} + A_{LL} = 0. \quad (12)$$

We have investigated a mechanism producing a large analyzing power in the energy range 28–50 GeV/ c . Let us discuss the energy dependence that we have found and ask: does this effect persist at high energy? In the impact picture we have $\Phi_1 \approx \Phi_3$ and $\Phi_2 \approx -\Phi_4$, and Φ_2 is smaller than Φ_1 . So A is essentially given by

$$A \approx (-\text{Im}\Phi_1 \text{Re}\Phi_5) / [(\text{Im}\Phi_1)^2 + 2(\text{Re}\Phi_5)^2], \quad (13)$$

where $\text{Im}\Phi_1$ is the imaginary part of the diffractive amplitude and $\text{Re}\Phi_5$ the real part of the flip QGD-ACD amplitude. In the large-angle region, it is known from the

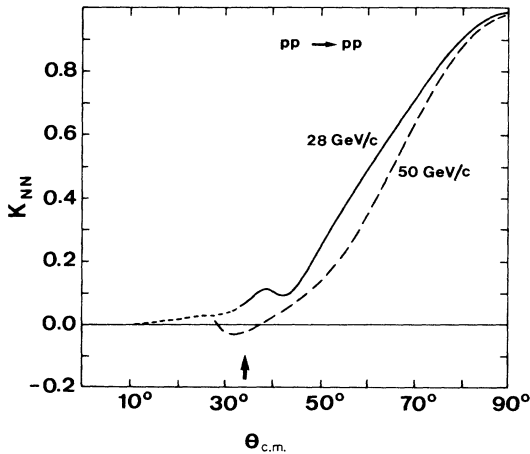


FIG. 8. Model predictions for K_{NN} vs $\theta_{c.m.}$ in p - p elastic scattering at $p_{lab}=28$ and 50 GeV/ c .

impact picture that $\text{Im}\Phi_1$ is negative⁷ while $\text{Re}\Phi_5$ given by the QGD-ACD is positive. As a result, A is positive. In the kinematic region under consideration, i.e., $\theta_{c.m.} > 45^\circ$ and

$$28 \text{ GeV}/c \leq p_{lab} \leq 50 \text{ GeV}/c,$$

since the QGD-ACD amplitude dominates, the ratio in Eq. (13) reduces to $-\text{Im}\Phi_1/\text{Re}\Phi_5$. At fixed angle, when the energy increases, since the hard-scattering contribution drops faster than the impact-picture amplitude, due to the $1/s^{9/2}$ factor, it is clear that A will increase. However, this behavior is limited because, as a result of the fast decrease of the QGD-ACD contribution, one will ultimately reach an energy where $\text{Im}\Phi_1$ dominates over $\text{Re}\Phi_5$ and the ratio of Eq. (13) will then become $-\text{Re}\Phi_5/\text{Im}\Phi_1$ which is going to zero for asymptotic energies. For example, we have checked numerically that at $p_{lab}=100$ GeV/ c and $\theta_{c.m.} \approx 20^\circ$ one has $A \approx 4\%$. Using the same arguments, one can understand the energy behavior of A_{NN} . We expect A_{NN} to decrease at fixed angle, because

$$A_{NN} \approx [(\text{Re}\Phi_i)^2 + \text{Im}\Phi_1 \text{Im}\Phi_2] / \sigma_0$$

and in the impact picture $\text{Im}\Phi_2$ is found positive.

III. SPIN EFFECTS IN PERTURBATIVE QCD

Perturbative QCD has achieved some success in the realm of short distance of physics, particularly in lepton-hadron scattering, large- p_T reactions, and so on. In the case of hadronic-exclusive processes the power-law scaling obtained for the energy dependence of the differential cross section confirms the ideas of asymptotic freedom and PQCD. Unfortunately, life is more complicated when calculating the angular dependence of the scattering amplitudes because one has to deal with a very large number of diagrams¹⁹ and a final result for nucleon-nucleon scattering is not yet available. As far as spin is concerned, the leading-twist contributions to the amplitudes are helicity conserving which implies for N - N elastic scattering that the amplitudes Φ_1 , Φ_3 , and Φ_4 are nonzero while Φ_2 and Φ_5 which are helicity-nonconserving must be zero. The constituent-interchange model gives for large angle the following real helicity amplitudes:²⁰

$$\begin{aligned} \Phi_1 &= \Phi_3 - \Phi_4, \Phi_2 = \Phi_5 = 0, \\ \Phi_3 &= 56F(\theta) + 68F(\pi - \theta), \\ \Phi_4 &= -68F(\theta) - 56F(\pi - \theta), \end{aligned} \quad (14)$$

with

$$F(\theta) = 0.5 / (1 - \cos\theta)^4.$$

This simple set of amplitudes gives $A_{NN}(90^\circ) = \frac{1}{3}$ in contradiction with the 12-GeV/ c data.² In addition, since $\Phi_5 = 0$, the mechanism described in Sec. II leads to a zero analyzing power. Of course one could use the mechanism in a different way by supposing that an interference occurs between the helicity conserving PQCD amplitudes and the single-flip diffractive amplitude Φ_5 . Unfortunately the argument does not work because the single-flip dif-

fractive amplitude is much smaller than the nonflip-diffractive amplitude at all angles and as a result A gets a negligible contribution from that at large angles. Clearly the modulus of the PQCD helicity-conserving amplitudes are constrained by the cross section so their size cannot be increased in order to compensate the smallness of the diffractive amplitudes.

Higher-order twist effects can be invoked to avoid these difficulties of PQCD but these corrections are unknown and only heuristic arguments for the relative size and phase have been discussed in Ref. 21. There one assumes that the relation $|\Phi_1| \approx |\Phi_3|$ is satisfied, also $\Phi_4 \approx -\frac{1}{2}\Phi_3$ (except at 90° , where $\Phi_4 = -\Phi_3$) and $\Phi_2 = 0$. The main difference with our model calculations is that we have $\Phi_2 \approx -\Phi_4$. With the present experimental value of $A_{NN}(90^\circ)$ at $p_{\text{lab}} = 12 \text{ GeV}/c$ one can accommodate $\Phi_2 = 0$ since one gets $A_{NN}(90^\circ) = \frac{2}{3}$ for $\Phi_1 = \Phi_3$. However if $A_{NN}(90^\circ)$ continues to increase with energy while $\Phi_2 = 0$ it would mean that Φ_1 must be larger than Φ_3 giving an unexpected result.²⁷ In that case $K_{NN}(90^\circ)$ should decrease with increasing energy while in our case it should remain of the order of $A_{NN}(90^\circ)$. Another experimental test of the assumption $\Phi_2 = 0$ is to measure $A_{SS}(90^\circ)$ and in that case we should get

$$A_{SS}(90^\circ) = -A_{NN}(90^\circ).$$

Concerning Φ_5 we find that in the angular range considered ($50^\circ - 70^\circ$), $|\Phi_5| \approx (\frac{1}{3} - \frac{1}{5})|\Phi_1|$ to be compared with $(\frac{1}{5} - \frac{1}{6})|\Phi_1|$ obtained in Ref. 21 with an arbitrary choice of the phase.

Beside these approaches different models are proposed in the literature to explain spin effects in large-angle elastic scattering.²²⁻²⁶ A simple parton interpretation of the observed large $A_{NN}(90^\circ)$ is proposed in Ref. 22. Large-angle p - p elastic scattering is due to the scattering of valence quarks carrying a large fraction x of the hadron momentum but the p - p and q - q scattering angles are in general different except when $x = 1$. They assume that only one quark from each proton is involved in the elementary subprocess and is allowed to change its momentum and spin directions while the others are spectators and conserve their spins. This is similar to our model but unlike our case they emphasize that most of the effects comes from the proton wave function and not from the nature of q - q scattering. Although A_{NN} is found to be the order of 60–70% at 90° and decreases for smaller angles, they predict $A = 0$ since $\Phi_5 = 0$ at all angles. In addition if one tries to calculate the differential cross section from this set of amplitudes²⁸ the angular dependence is in-

correct which is a serious drawback of the model. This last difficulty is absent in Ref. 23, where a calculation of p - p elastic scattering based on the idea of the end-point dominance in leading order with one-gluon exchange leads to a fair description of the angular distribution and a large positive A_{NN} , although one still finds $\Phi_5 = 0$.

Finally let us recall that there is some evidence for an oscillatory pattern with energy of the p - p elastic cross section at 90° , which can be explained in terms of the chromo-Coulomb phase shift.²⁴ It is conceivable that some spin observables at fixed angle oscillate as well.²⁵ This is also predicted in an approach based on a quantum field three-dimensional dynamical equation (Ref. 26). A_{NN} oscillates around the value $\frac{1}{3}$ for $\theta_{\text{c.m.}} = 90^\circ$ and a large analyzing power at large angles can be obtained by adjusting the relative phase between flip and nonflip amplitudes through a free parameter which is related to the fraction of energy carried by valence quarks.

IV. CONCLUDING REMARKS

We have presented an interference mechanism between the diffractive spin-nonflip amplitude and the hard QGD-ACD amplitudes which can explain the rapid increase of the analyzing power in large-angle p - p elastic scattering at medium energy. We would like to stress that the sets of amplitudes we use in the calculation were fixed before we analyzed the consequences of this mechanism, so all our results are pure predictions which do not require to adjust any free parameter. The crucial role of spin in large-angle meson-baryon scattering has also been emphasized following the QGD-ACD approach and its confrontation with experimental observations is presented in Ref. 29.

A comparison with pure perturbative QCD is difficult because reliable results are not available at the moment. Nevertheless expectations derived from heuristic arguments exhibit some differences with our approach at the level of the relative size of the amplitudes and on the behavior of spin correlation parameters. The experimental program in progress at Brookhaven National Laboratory will be of a great help to clarify the situation in this fascinating field of particle physics.

ACKNOWLEDGMENT

J.S. wishes to acknowledge the hospitality of the theory group at Brookhaven National Laboratory where this work has been completed. Centre de Physique Théorique is Laboratoire Propre du CNRS.

¹A. Yokosawa, Phys. Rep. **64**, 47 (1980).

²R. Fernow and A. Krisch, Annu. Rev. Nucl. Sci. **31**, 107 (1981).

³C. Bourrely, J. Soffer, and E. Leader, Phys. Rep. **59**, 95 (1980).

⁴D. Peasle *et al.*, Phys. Rev. Lett. **50**, 802 (1983); **51**, 2359 (1983); P. Cameron *et al.*, Phys. Rev. D **32**, 3070 (1985).

⁵G. Court *et al.*, Phys. Rev. Lett. **57**, 507 (1986).

⁶H. Miettinen *et al.*, Phys. Rev. D **16**, 549 (1977); J. O'Fallon *et al.*, Phys. Rev. Lett. **39**, 733 (1977).

⁷C. Bourrely, J. Soffer, and T. T. Wu, Phys. Rev. D **19**, 3249 (1979).

⁸C. Bourrely, J. Soffer, and T. T. Wu, Nucl. Phys. **B247**, 15

- (1984).
- ⁹C. Bourrely, H. Neal, H. Ogren, J. Soffer, and T. T. Wu, Phys. Rev. D **26**, 1781 (1982).
- ¹⁰G. Preparata, in *Lepton and Hadron Structure*, proceedings of the 1974 Erice Summer School, edited by A. Zichichi (Academic, New York, 1975), p. 54; G. Preparata and N. Craigie, Nucl. Phys. **B102**, 478 (1976); G. Preparata and K. Szego, Phys. Lett. **68B**, 239 (1979); Nuovo Cimento **47A**, 303 (1978); G. Preparata, Nucl. Phys. **B122**, 29 (1977).
- ¹¹A preliminary version of the underlying mechanism was presented in C. Bourrely and J. Soffer, Phys. Rev. Lett. **54**, 760 (1985).
- ¹²G. Preparata and J. Soffer, Phys. Lett. **86B**, 304 (1979); P. Chiapetta and J. Soffer, Phys. Rev. D **28**, 2162 (1983).
- ¹³G. Nardulli, G. Preparata and J. Soffer, Nuovo Cimento **83A**, 361 (1984).
- ¹⁴G. Nardulli, G. Preparata and J. Soffer, Phys. Rev. D **31**, 626 (1985).
- ¹⁵J. Allaby *et al.*, Nucl. Phys. **B52**, 316 (1973).
- ¹⁶The Coulomb-nuclear interference at very small momentum transfer exhibits a similar phenomena. A. Vanzha, L. Lapidus, and A. Tarasov, Yad. Fiz. **16**, 1023 (1972) [Sov. J. Nucl. Phys. **16**, 565 (1973)]; B. Kopeliovich and L. Lapidus, *ibid.* **19**, 218 (1974) [**19**, 114 (1974)].
- ¹⁷Z. Asa'd *et al.*, Nucl. Phys. **B255**, 273 (1985).
- ¹⁸Y. Makdisi *et al.*, Phys. Rev. Lett. **45**, 1529 (1980).
- ¹⁹G. Farrar, Phys. Rev. Lett. **53**, 28 (1984).
- ²⁰G. Farrar, S. Gottlieb, D. Sivers, and G. Thomas, Phys. Rev. D **20**, 202 (1979); S. Brodsky, C. Carlson, and H. Lipkin, *ibid.* **20**, 2278 (1979).
- ²¹G. Farrar, Phys. Rev. Lett. **56**, 1643 (1986).
- ²²M. Anselmino, Z. Phys. C **13**, 63 (1982).
- ²³J. Szwed, Phys. Lett. **93B**, 485 (1980); Acta Phys. Pol. **B14**, 239 (1983).
- ²⁴B. Pire and J. Ralston, Phys. Rev. Lett. **49**, 1605 (1982).
- ²⁵A. W. Hendry, Phys. Rev. D **23**, 2075 (1981).
- ²⁶S. Troshin and N. Tyurin, *Proceedings of the Second International Workshop on High Energy Spin Physics, Protvino, 1984*, edited by Soloviev *et al.* (Serpukhov, 1985), p. 229; Fiz. Plazmy **15**, 53 (1984) [Sov. J. Part. Nucl. **15**, 25 (1984)].
- ²⁷Another consequence of the assumption $\phi_1 = \phi_3$ is the fact that the spin asymmetry A_{LS} defined in Ref. 3 is expected to be very small. This is in agreement with experimental observation. See P. Auer *et al.*, Phys. Rev. D **34**, 1 (1986), and references therein.
- ²⁸We thank M. Anselmino for providing us his results. Recently he has informed us that, due to an inconsistent use of spin-rotation conventions, the result of Ref. 22 on a large A_{NN} near 90° is no longer valid.
- ²⁹G. Preparata and J. Soffer, Phys. Lett. B (to be published).